Interdiffusion in Polystyrene and End-Functional Polystyrene Thin Films near a Solid Surface

Chia-Ying Wang[1], Vivek M. Prabhu[1], Christopher L. Soles[1], Bryan D. Vogt[1], Wen-li Wu[1], Eric K. Lin[1] and Sushil K. Satija[2]

[1]Polymers Division, National Institute of Standards and Technology, Gaithersburg, MD 20899

[2]Center for Neutron Research, National Institute of Standards and Technology, Gaithersburg, MD 20899

INTRODUCTION

Understanding polymer dynamics and thermal properties in thin films is pertinent because many technologies rely on performance in small length scales. For example, dimensional control approaches the molecular scale in polymeric photoresist materials for the development of sub-100 nm features in the semiconductor industry. For polymer thin films, the free surface (polymer/air interface) and solid surface (polymer/substrate interface) have been shown to affect the glass transition temperature, T_g, significantly.[1,2] In this work, interdiffusion of polystyrene (PS) chains near a silicon oxide surface is investigated using neutron reflectometry. The effective diffusion coefficient, D_{eff}, an estimation of polymer interdiffusion rate, is obtained as a function of film thickness. In addition, similar measurements are performed on α,ω-dicarboxy terminated polystyrene ($PS(COOH)_2$) thin films, where the carboxyl end group interacts strongly with the silanol group present in the silicon oxide layer. D_{eff} of PS deviates from the bulk value when the film thickness is less than 200 Å, which is approximately two times the bulk radius of gyration, R_g. For $PS(COOH)_2$, D_{eff} is smaller than that of PS in similar thickness, possibly due to the more favorable polymer/substrate interaction and hydrogen bonding between chain ends themselves.

EXPERIMENTAL

Materials. Hydrogenated polystyrene, hPS ($M_{r,w}$ = 99,800 g/mol), α,ω-dicarboxy terminated polystyrene, $hPS(COOH)_2$ ($M_{r,w}$ = 100,400 g/mol), and fully deuterated polystyrene (d_8), dPS ($M_{r,w}$ = 100,300 g/mol), were used as received. Using DSC with a heating rate of 10 ºC/min, the glass transition temperature T_g was determined to be 105 ºC, with a standard uncertainty of 2 ºC, for both hPS and $hPS(COOH)_2$ and 95 ºC ± 2 ºC for dPS. The radius of gyration, R_g, is estimated to be 94 Å for all of the polymers since they have similar molecular weight.

Bilayer samples were prepared on polished, 3 mm thick, silicon wafers. A silicon oxide layer with controlled thickness of 5 Å to 10 Å was formed on the wafer in a UV/ozone cleaner, after the native oxide surface was etched using a buffered hydrofluoric acid solution. Various thickness of hPS and $hPS(COOH)_2$ thin films were spin coated on the wafer from 0.1 % to 2.0 % mass fraction toluene solutions. The hydrogenated layers were annealed under vacuum at 180 ºC for 17 h. The overlaid dPS was first spin coated on a glass slide from a toluene solution of mass fraction 1.8 % and transferred onto of the hydrogenated layer using the typical floating method. The thickness of the top layer was determined by neutron reflectometry and averaged around 800 Å (765 Å ± 2 Å to 822 Å ± 2 Å); a detailed description is given in the next section. The final bilayer samples were dried under vacuum at room temperature for 17 h. For interdiffusion measurements, each bilayer sample was annealed under vacuum at 120 ºC for various times. Following each annealing, the sample was quickly quenched to room temperature by placing it on a large aluminum block (less than 30 s). The neutron reflectivity measurement was then conducted at room temperature; interdiffusion is halted as the temperature is well below the bulk T_g.

Neutron Reflectivity. The neutron reflectivity measurements were performed using NG-7 reflectometer at the Center for Neutron Research, National Institute of Standards and Technology. The wavelength of the neutrons, λ, is 4.768 Å, and the scattering vector, q, is equal to $(4\pi/\lambda)\sin\theta$, where θ is the incident angle. The reflectivity is obtained as a function of q and is sensitive to the profile of the neutron scattering length density perpendicular to the sample surface. Accordingly, the scattering length density is the physical quantity used in determining the concentration profile. The values for hPS, dPS, and silicon are (1.42×10^{-6}) $Å^{-2}$, (6.47×10^{-6}) $Å^{-2}$, and (2.11×10^{-6}) $Å^{-2}$, respectively, and $hPS(COOH)_2$ is assumed to have the same scattering length density as hPS. The concentration profile of the bilayer is determined by first generating a model profile and fitting the calculated reflectivity to the measured reflectivity data through the recursive method, applying the nonlinear least-squares principle.

RESULTS AND DISCUSSION

Figure 1(a) presents the neutron reflectivity data with the best fit curves for the hPS/dPS bilayer with the hPS thickness of 393 Å. The reflectivity profile of the initially prepared sample (as cast) consists of many distinct interference fringes, indicating a sharp interface between two layers. The spacing of these fringes is determined by the thickness of the top dPS layer. Reflectivity data at two annealing times are also shown, shifted for clarity. As the sample is annealed at 120 ºC, the interface between the layers broadens due to polymer movement, resulting in the diminution of the higher order peaks at larger q values. Similar results are observed for $hPS(COOH)_2$/dPS bilayers, which are not shown here. The dampening of the higher order fringes at long annealing times in $hPS(COOH)_2$/dPS bilayers is not as significant as that in hPS/dPS bilayers with similar thickness. Figure 1(b) displays the real space profile of the scattering length density obtained from the best fits to the corresponding reflectivity data in Figure 1(a). In general, an error function is utilized to describe the interfacial profile. The abscissa denotes the distance from the silicon surface. The profile shows a steep change between hPS and dPS layers initially (solid line) and the width of interface increases as the sample is annealed at 120 ºC for 9 min (dotted line) and 165 min (dashed line).

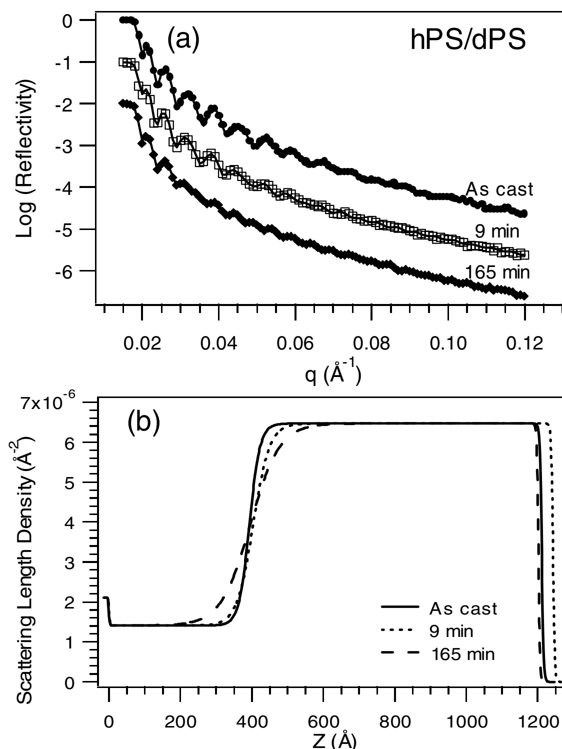

Figure 1. (a) Neutron reflectivity of the hPS/dPS bilayer (thickness: 393/818 Å) as a function of the scattering vector q, as the sample is initially prepared and annealed at 120 ºC for 9 min and 165 min. The standard uncertainty in the data is comparable to the size of the symbols. (b) Real space profiles obtained from the best fits to the reflectivity data, which are shown as the solid curves in (a).

The interfacial width between the hydrogenated and deuterated layers, σ, is determined by calculating the half-width at half of the maximum of the derivative of the scattering length density profile. The initial width of the as-cast samples, σ_0, ranges from 5 Å to 15 Å, attributed to the residual roughness from the sample preparation and capillary fluctuations. The interfacial width at subsequent annealing times is then subtracted quadratically by σ_0, $\Delta\sigma = (\sigma^2 - \sigma_0^2)^{1/2}$. In Figure 2, the corrected interfacial widths, $\Delta\sigma$, of each hPS/dPS sample (Figure 2(a)) and hPS(COOH)$_2$/dPS sample (Figure 2(b)) are plotted as a function of the square root of the annealing time, $t^{1/2}$. The thickness of the bottom layer determined from the best fit (standard uncertainty 2 Å) is listed in the legend.

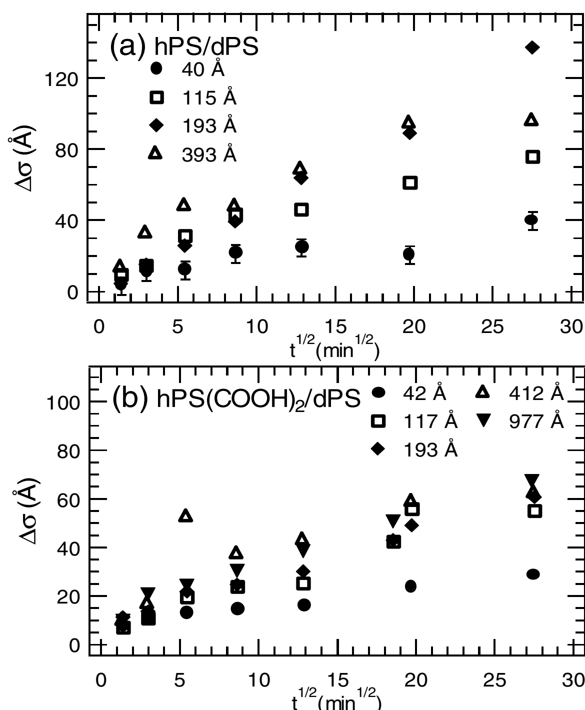

Figure 2. Interfacial width $\Delta\sigma$ plotted as a function of the square root of the annealing time at 120 ºC for (a) hPS/dPS bilayers with varying hPS layer thickness and (b) hPS(COOH)$_2$/dPS bilayers with varying bottom layer thickness. The error bars, indicating the standard uncertainty in the value of $\Delta\sigma$, are similar for all the samples and only shown for one set of data for clarity.

In Figure 2(a), a $t^{1/2}$ dependence of $\Delta\sigma$ is observed at long annealing times for thicker hPS/dPS samples, signifying normal Fickian diffusion behavior. When the bottom layer becomes thinner, the dependence of $\Delta\sigma$ on annealing time becomes weaker. These results indicate that during a similar annealing time, polystyrene chains in thin films move far less than those in thicker films. These chains are constrained by the silicon substrate or energetically slowed down due to the weakly attractive interaction between polystyrene and the silicon oxide surface. Meanwhile, motion of polystyrene chains is further retarded when the polymer-substrate interaction is more favorable, as for the system of hPS(COOH)$_2$/dPS shown in Figure 2(b). Fickian diffusion ($\Delta\sigma \sim t^{1/2}$) is not recovered even for the thickest hPS(COOH)$_2$/dPS sample at long annealing times. Nevertheless, to facilitate the characterization of the interdiffusion rate, the data in Figure 2 are linearly fit over the entire time scale and the slope of the best fit is used to calculate an effective diffusion coefficient D_{eff}. For most samples studied here, D_{eff} is not strictly the bulk diffusion constant, instead, it is an effective segment diffusion constant that averages over different modes of dynamics.

Figure 3 summarizes the D_{eff} obtained for both hPS/dPS and hPS(COOH)$_2$/dPS systems as a function of the initial bottom layer thickness normalized by the bulk R_g. The bulk diffusion coefficient, D_{bulk}, for a polystyrene of 100,000 g/mol molecular weight at 120 ºC is shown in the region indicated by dashed lines. These estimations are calculated from literature values considering the $D \sim M^{-2}$ relationship and applying the Vogel equation for the temperature dependence of D.[3,4] In hPS/dPS bilayers, D_{eff} deviates from D_{bulk} when the film thickness is less than 2 R_g, suggesting that the confinement effect imposed by the silicon substrate only extends to a distance comparable to the chain dimension. These results are consistent with the observation in poly(methyl methacrylate) thin films, where the substrate affected the polymer mobility up to ≈ 3 R_g.[5] In contrast, it has been reported that long-range effects of solid substrate (up to 10 R_g) were observed in polystyrene diffusion using secondary ion mass spectrometry.[6] In the higher interfacial energy system studied here, D_{eff} of hPS(COOH)$_2$/dPS seems to reach its asymptotic value when the film is 2 R_g thick. Moreover, D_{eff} stays smaller than D_{bulk} of polystyrene even in the thicker films. Hydrogen bonding between carboxyl end groups could slow down polymer dynamics. Comparing D_{eff} obtained for both polymers having the film thickness near 4 R_g, a ratio of 4.5 supports the explanation that the dimerization of hPS(COOH)$_2$ chains may occur during the annealing and hence reduce chain mobility.

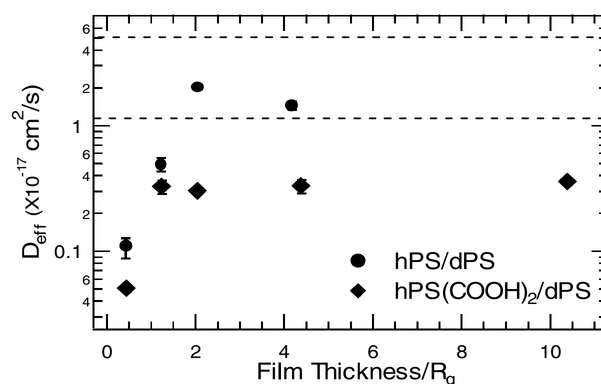

Figure 3. Effective diffusion constant D_{eff} as a function of the initial bottom layer thickness normalized by the bulk R_g. The dashed lines indicate the range of estimated bulk diffusion coefficient for a 100,000 g/mol molecular weight polystyrene at 120 ºC. The error bars denoting the standard uncertainty in D_{eff}, if not visible, are smaller than the size of the data symbols.

CONCLUSIONS

Interdiffusion in hPS/dPS and hPS(COOH)$_2$/dPS bilayers prepared on silicon substrates are studied using neutron reflectometry. The effective diffusion coefficient D_{eff} deviate from the bulk rate when the thickness of the hPS bottom layer is less than 2 R_g. D_{eff} measured in hPS(COOH)$_2$/dPS samples are all lower than those in hPS/dPS bilayers with similar film thickness and reach an asymptotic value when the bottom layer is 2 R_g thick. These results suggest that the confinement effect of the silicon substrate only extends to a distance comparable to the molecular dimension. The strong interaction between the carboxyl end group of hPS(COOH)$_2$/dPS and the silanol group present in the silicon oxide layer as well as hydrogen bonding between chain ends themselves slow down polymer movement.

REFERENCES

1. Forrest, J. A.; Dalnoki-Veress, K.; Dutcher, J. R. *Phys. Rev. E* **1997**, *56*, 5705.
2. Fryer D. S.; Peters, R. D.; Kim, E. J.; Tomaszewski, J. E.; de Pablo, J. J.; Nealey, P. F.; White, C. C.; Wu, W.-l. *Macromolecules* **2001**, *34,* 5627.
3. Green, P. F.; Kramer, E. J. *J. Mater. Res.* **1986**, *1*, 202.
4. Whitlow, S. J.; Wool, R. P. *Macromolecules* **1991**, *24*, 5926.
5. Lin, E. K.; Wu, W.-l.; Satija, S. K. *Macromolecules* **1997**, *30*, 7224.
6. Zheng, X.; Rafailovich, M. H.; Sokolov, J.; Strzhemechny, Y.; Schwarz, S. A.; Sauer, B. B.; Rubinstein, M. *Phys. Rev. Lett.* **1997**, *79*, 241.